Mitigating cerium migration for perfluorosulfonic acid membranes using organic ligands

Agarwal, Tanya; Gonzales, Ivana; Adhikari, Santosh; Park, Eun Joo; Komini Babu, Siddharth; Kim, Yu Seung; Tian, Ding; Bae, Chulsung; Oscar, Morales-Collazo; Joan, F. Brennecke; Prasad, Ajay K.; Advani, S. G.; Sievert, Allen; Park, Andrew; Hopkins, Timothy; Borup, Rodney L.

To be published in: Journal of Power Sources

DOI to publisher's version: 10.1016/j.jpowsour.2022.232320

Mitigating Cerium Migration for Perfluorosulfonic Acid Membranes using Organic Ligands

Tanya Agarwal,[1,2] Ivana Matanovic,[3,4] Santosh Adhikari,[1] Eun Joo Park,[1] Siddharth Komini Babu,[1] Yu Seung Kim,[1,*] Ding Tian,[5] Chulsung Bae,[5] Oscar Morales-Collazo,[6] Joan F. Brennecke,[6] Ajay K. Prasad,[2] Suresh G. Advani,[2] Allen Sievert,[7] Timothy Hopkins,[7] Andrew Park,[7] and Rod Borup[1,**]

[1]MPA-11: Materials Synthesis & Integrated Devices, Los Alamos National Laboratory, Los Alamos, NM 87545, USA

[2]Center for Fuel Cells and Batteries, Department of Mechanical Engineering, University of Delaware, Newark, DE 19716, USA

[3]Department of Chemical and Biological Engineering, Center for Micro-Engineered Materials (CMEM), The University of New Mexico, Albuquerque, NM 87231, USA

[4]Theoretical Division, Los Alamos National Laboratory, Los Alamos, NM 87545, USA

[5]Department of Chemistry and Chemical Biology, Rensselaer Polytechnic Institute, Troy, NY 12180, USA

[6]McKetta Department of Chemical Engineering, The University of Texas at Austin, Austin, TX 78712, USA

[7]The Chemours Company, Newark, DE 19713, USA

*Correspondence: yskim@lanl.gov, borup@lanl.gov

Abstract

Improving the electrochemical stability of proton exchange membranes is a pressing priority for heavy-duty fuel cell vehicles. The lifetime of the most widely used perfluorosulfonic acid membranes is limited by reactive free radicals generated inside the system. Cerium has been found to reduce the chemical degradation of the membranes. However, cerium migration during fuel cell operation limits the chemical durability enhancement effect expected from the radical scavenging activity of cerium. Here we investigate a wide range of organic immobilizers for cerium, measuring their suitability concerning cerium retention, radical scavenging activity, and fuel cell performance. We report that partially fluorinated phosphonic acids enhance cerium retention up to 45 times and reduce fluoride emission rate by 38% compared to the commercial Nafion™ XL membrane pre-impregnated with cerium. The energetics of cerium-phosphonic acid complex systems by density functional theory calculations rationalizes effective cerium immobilization.

Keywords: Proton exchange membrane fuel cell; perfluorosulfonic acid; chemical stability; durability; cerium migration; radical scavenger

1. Introduction

Polymer-electrolyte membrane fuel cells (PEMFCs) are an attractive technology to power zero-emission vehicles. As fuel cells extend to heavy-duty vehicle (HDV) applications, improving the stability of proton exchange membranes (PEMs) becomes the most demanding requirement.[1] According to the US DOE's multi-year research, development, and demonstration plan, PEMFCs require a 30,000-hour lifetime for HDV applications.[2]

Perfluorosulfonic acid (PFSA) polymers such as Nafion™ are state-of-the-art PEMs, and their chemical degradation is triggered by reactive free radical species. Small amounts of reactant gases crossing over through the membrane generate hydroxyl radicals, which attack the main chain and side chain of PFSAs under fuel cell operating conditions.[3] The degradation rate of PEMs increases when radical generation is catalyzed by metal ion impurities such as iron, copper, and titanium present in the membrane electrode assembly (MEA).[4] To mitigate the degradation of PFSA, cerium has been used as a free-radical scavenger since the mid-2000s.[5] The free radical scavenging rate of cerium is much higher than those of other inorganic radical scavengers,[6] making it the widely used additive in commercial membranes.

Cerium below 0.6 wt% in Nafion™ was found to increase the chemical stability of PFSA by three orders of magnitude over the non-modified Nafion™.[7] The open-circuit voltage (OCV) degradation rate under accelerated stress testing for cerium-incorporated membrane was 50 $\mu V\ hr^{-1}$ vs. 1000 $\mu V\ hr^{-1}$ for a membrane without cerium.[7] However, cerium ions are highly mobile due to diffusion under a concentration or potential gradient, gradually losing their efficacy as a radical scavenger.[8] [9] Cerium migration has been observed between the catalyst layers and in the active and inactive areas of the membrane during cell discharge.[10] Baker et al. [11] observed that the migration of cerium is highest at high charge transfers and highly humidified conditions. Lai et al. [12] found in their highly accelerated stress tests that the degradation of PFSA was highest in regions that were deprived of cerium.

Several approaches to mitigate the loss of cerium ions have been suggested. The first approach is to increase cerium concentration in the catalyst layer or membrane to counteract the loss of cerium.[7, 13] However, a high cerium content substantially compromises the proton conductivity of the membrane. The second approach is using cerium oxide[14] or mixed metal oxides such as cerium zirconium oxide nanoparticles or nanofibers[15, 16] by utilizing the change in the crystalline structure of cerium to delay the dissolution time of cerium ions. Embedding cerium into graphene oxides[17] or titanium

carbide[18] is another strategy, however, the reduction of proton conductivity and embrittlement of PFSAs with embedded cerium nanoparticles remains a concern. The incorporation of organic ligands to immobilize cerium ions is an alternative approach. Organic compounds can be molecularly dispersed in PFSAs without sacrificing the mechanical properties of the membranes. Marta et al. found [19] increased resistance to radical attack for Aquivion™ membranes incorporated by halloysites. Crown ethers have been suggested to immobilize cerium ions,[20, 21] [22] but little, if any, evidence of stabilization was provided nor were other property changes from incorporation investigated. A recent study by Agarwal et al. showed improved retention of cerium and higher durability of PFSA with the incorporation of appropriate size of crown ethers [23].

Here we explore several organic cerium immobilizers for their ceric retention efficiency. The organic ligands include crown ether, phosphine oxide, phosphonate ester, phosphinic/phosphonic acid, carboxylic acid, amine, and ammonium hydroxide. The cerium retention mechanisms of promising organic ligands are investigated by density functional theory (DFT) calculations. The optimal ligands are then evaluated for practical use in fuel cells in terms of the radical scavenging efficiency of cerium after complex formation, membrane homogeneity, proton conductivity, and catalyst poisoning. This study aims to motivate a molecular design strategy of cerium stabilizers for enhancing the lifetime of cerium in PFSA-based PEMs, thereby enhancing the durability of fuel cells for HDVs.

2. Results and Discussion

2.1 Structural Effects of Organic Ligands on Ceric Retention

2.1.1 Functional groups

Organic ligands used for lanthanide extraction were selected to evaluate the ceric retention (CR). Table 1 (a full list can be found in Table S1) compares the CR of crown ether, phosphinic/phosphonic acid, phosphine oxide, carboxylic acid, amine, and ammonium hydroxide with the functional group (FG) to the ceric ratio (FG/Ce) of 4. For di-phosphonic acids, two ligand molecules are used per ceric ion for FG/Ce=4. The baseline membrane (Ce-Nafion™) without an immobilizing additive showed insignificant CR. The CR for crown ethers was found to depend on the size of the cavity of the crown ether. The CR for various crown ethers followed the order 15-crown-5 > 12-crown-4 > 18-crown-6. 15-Crown-5 (15C5) showed a 2.4-fold higher CR than the baseline membrane after 24 hr. The cavity size of 15C5 is closest to the cerium ion[24] likely causing higher CR. Aminomethyl-15-crown-5 (A-15C5) showed comparable CR to the unsubstituted 15C5. Benzo-15-crown-5 (B-15C5), on the other hand, showed much lower CR,

possibly due to the rigidity of the crown ether that inhibits forming of stable complexes with the ceric ion.[25] Cyanex® 923, a mixture of 19 alkyl phosphine oxides, showed the highest CR, which supports its extensive use as a cerium extracting agent.[26] Phosphonic acids showed relatively high CR, but the retention for the acid ligands is a strong function of the structure. For example, (12-phosphonododecyl) phosphonic acid (PDPA) was 58.6%, approximately 90% higher than the shorter chain counterpart octane di-phosphonic acid (ODPA). Mono-phosphonic acids such as fluoro-octylphosphonic acid (PFOPA) and fluoro-dodecylphosphonic acid (FHPA) showed higher CR than the di-phosphonic acid being similar chain length molecules. Phosphinic acid and phosphonate ester showed relatively low CR, and perfluorinated carboxylic acids show minimal CR (< 3.5%). All amine and ammonium hydroxide ligands did not show any CR, even lower than the Ce-Nafion™ baseline membrane. This could result from the protonation of these ligands under an acidic environment, which in turn interact more favorably with the $-SO_3^-$ in Nafion™ rather than binding with cerium. The high solubility of these ligands in water could be another reason. The preliminary screening of the ligands showed that phosphinic acid, esters, carboxylic acids, ammonium, and amine base ligands are ineffective as complexing agents for cerium in the PFSA environment and therefore not investigated further. It is note that some of the chelating agents that failed in our ex-situ tests might work in an operating fuel cell, but the current tests were aimed at screening true positives.

Table 1. CR of ligands from the selected categories

No.	Category	Name[a]	Chemical structure of organic ligand	CR (%)[b]
1	Baseline	Ce-Nafion™	None	2.0 [3.2]
2	Crown ether	15C5		4.8 [17.6]
3	Phosphonate ester	POE		5.0
4	Phosphinic acid	DPPA	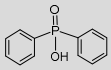	6.0
5	Phosphonic acid	PFOPA	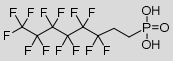	35.7
6	Phosphonic acid	PDPA	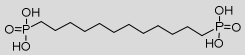	58.6
7	Phosphine oxide	Cyanex® 923	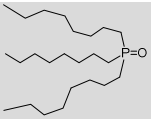	88.3

8	Carboxylic acid	HIFUA		3.4
9	Amine	Melanin	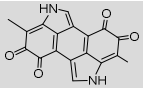	0.0 [2.2]
10	Ammonium hydroxide	TEAOH		0.0 [3.6]

[a]15C5: 15-crown-5; POE: (heptadecafluorooctyl)phosphonate diethyl ester; DPPA: diphenylphosphinic acid; PFOPA: 1H,1H,2H,2H-perfluorooctanephosphonic acid; PDPA: (12-phosphonododecyl) phosphonic acid; HIFUA: Heneicosafluoroundecanoic acid; TEAOH: tetraethylammonium hydroxide.

[b]measured by X-ray fluorescence after 48 hours of the treatment in 0.5 M H_2SO_4 at room temperature; numbers in box brackets: CR after 24 hours of the treatment.

Next, we investigate the effect of the FG/Ce ratio on CR for crown ether and phosphonic acid ligands. Figure 1a shows that the CR of crown ethers did not change significantly with the FG/Ce ratio, suggesting that additional crown ethers are likely not interacting with cerium. On the other hand, the CR of phosphonic acids strongly depends on the FG/Ce ratio (Figure 1b). Among all phosphonic acid ligands investigated, phosphonic acids with FG/Ce=6 outperform others, suggesting that a high retention rate is associated with the coordination stoichiometry of cerium ions.

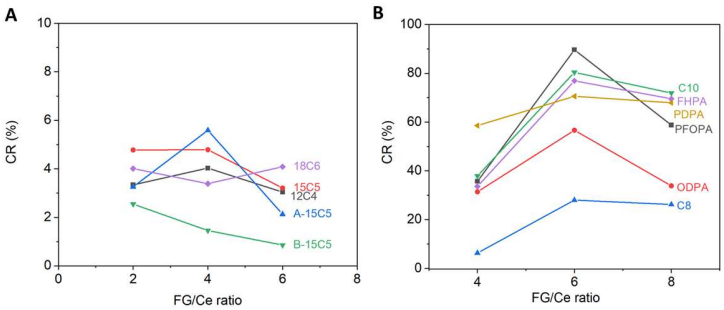

Figure 1. Effect of FG/Ce ratio on CR

CR of Ce-Nafion™ membrane having crown ethers (A) and phosphonic acids (B) as a function of FG/Ce ratio. C8: (heptadecafluorooctyl)phosphonic acid; C10: (henicosafluorodecyl)phosphonic acid; FHPA: P-(3,3,4,4,5,5,6,6,7,7,8,8,9,9,10,10,11,11,12,12,12-heneicosafluorododecyl)phosphonic acid; ODPA: octanediphosphonic acid.

2.1.2 Energetics of ceric-ligand complexes

The CR mechanisms by organic ligands have been investigated in the selective extraction and separation of lanthanum. For crown ethers, a cerium ion is coordinated to form a complex within a crown ether ring. It is known that the stability constants for crown ether complexes are governed by the cavity size and enthalpy changes from ion-dipole interactions.[27] The selective extraction mechanism

of lanthanum by phosphinic/phosphonic acids strongly depends on the ligand structure and the coordination number of ions. The pK_a of acid to release acidic proton and exchange with cerium cation is critical[28] through complexation with acid.[29] For these types of ligands, the tendency to form stable complexes with cerium, which is a hard Lewis acid cation, is the determining factor rather than their pK_a.[30]

The energetics of Ce-organic ligand complexes was investigated to prove the CR mechanisms. Figure 2a shows the optimized geometries for the ceric-crown ether complex at the FG/Ce ratio of 1 and 2. The DFT calculation indicated that coordination of more than two crown ether units to ceric is not possible due to steric effects. At a 2:1 ratio of crown ether to ceric ion, the ceric ion is completely coordinated. This result suggests that a minor increase in CR with increasing crown ether to cerium ratio is not caused by increased complex stability but likely by changes in the membrane properties. Figure 2b shows the optimized geometries for the C8 phosphonic acid-ceric complex as a function of the FG/Ce ratio. For FG/Ce=2, the complex structure could not be optimized, and therefore the interaction energy was evaluated by adding water molecules to complete the coordination shell of the ceric ion. Higher interaction energy was obtained with FG/Ce=4. Interaction energy for ceric with phosphonic acids increased by 29.5% from 1734.4 to 2246.6 kcal mol^{-1} when the FG/Ce ratio increased from 2 to 4. The phosphonic acid with FG/Ce=4 is also expected to have more water molecules co-occupying the inner coordination shell of the ceric, thereby dropping the stability of ceric ions in the acid solution when the water could be ultimately replaced by sulfates. The interaction energy further increased by 17% to 2621.6 kcal mol^{-1} when the FG/Ce ratio increased to 6 and completely occupied the inner shell, which explains the sharp jump in CR observed going from the FG/Ce ratio of 4 to 6 for almost all phosphonic acid ligands investigated. At FG/Ce=6, neither water nor sulfonic acid groups could replace phosphonic acid moieties, which artifacts as high cerium retention. The interaction energies for FG/Ce=8 could not be calculated due to the fully occupied shell of the complex at FG/Ce = 6, leaving no sites for further association with the larger ligands. The interaction energy of the C8-ceric cluster (FG/Ce=6) is 2.4-fold higher than that of the 15C5-ceric cluster (FG/Ce=2), explaining the marked increase in CR from crown ether to phosphonic acids. The higher ceric cluster energy with the C8 ligand is because the ion-pair interaction between the phosphonate and cerium ion (374.5 kcal mol^{-1} per Ce-O bond) is stronger than the dipole-ion interaction between the ether and cerium ion (109.9 kcal mol^{-1} per Ce-O bond), consistent with previous energetics study in phosphate-quaternary ammonium ion pairs.[31, 32] [33] In addition, the complexes of cerium ions and phosphonic acids are stabilized by hydrogen bonds that

form between acid P-OH and acid P=O/-CF_2 groups of neighboring ligands which further prevent cation exchange in the reaction medium. Figure 2c shows the optimized structures for trimethyl and triethyl phosphine oxide at FG/Ce=4 with and without water molecules. The interaction energy of triethyl phosphine oxide-ceric at the 4:1 ratio was 1179.3 kcal mol^{-1} which was 52% of the C8-ceric interaction energy at the given FG/Ce ratio. Adding four water molecules to the phosphine oxides increased the cluster interaction energy by ~ 100 kcal mol^{-1}. The interaction energy for crown ether and phosphine oxides is within 7%, but the CR for crown ether is a fraction of phosphine oxide. Phosphine oxides have lower interaction energy than phosphonic acids but higher CR, which suggests that the CR for phosphine oxides could not be explained by interaction energy alone and comes from factors not tapped in the DFT investigation.

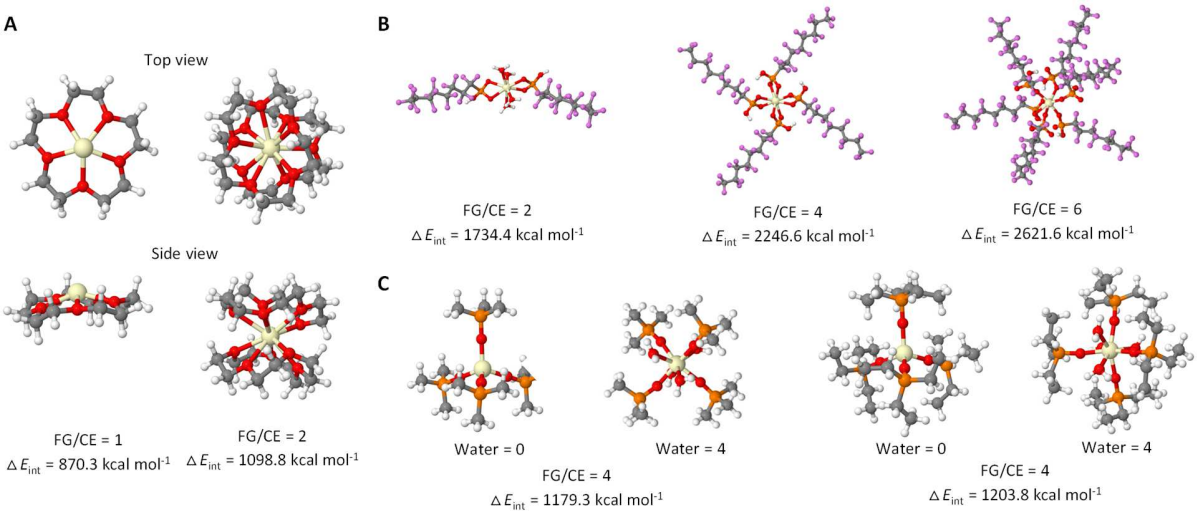

Figure 2. DFT optimized structures and interaction energies

(A) Ce-15C5 crown ether, (B) Ce-C8 phosphonic acid, and (C) Ce-trimethyl phosphine oxide (left) and triethyl phosphonie oxide (right). O – red, H – white, C – grey, Ce – yellow, and F – pink.

2.1.3 Effect of substituent of phosphonic acids on CR

The effect of the chain length of phosphonic acid ligands is investigated using house-made perfluorinated phosphonic acids with a chain length from 4 to 12 (Table S2). Phosphonic acids with a fluoroalkyl chain length of ≤ 6 showed low CR (< 5%), and the maximum CR was obtained with C10 (> 70%) (Figure 3A). This can be attributed to the solubility effect; phosphonic acids with a chain length of ≤ 6 have high solubility in water and are easily washed out from the membranes during the CR experiment, while the phosphonic acids with chain length ≥ 8 have substantially lower solubility in

water. It could also be related to the interaction of these ligands with the PFSA. Longer chain length ligands are likely to interact strongly with the Nafion™ backbone resulting in higher chain entanglement. Stronger PFSA ligand interaction would result in increased stability of ligands under an acidic environment. Di-phosphonic acids show similar effects with C4 bisphosphonic acid (C4DPA), showing much lower CR, 4%, than less soluble C8 and C12 alkyl di-phosphonic acids (ODPA, PDPA). Although phosphonic acids with higher chain lengths become less soluble in water, increasing the chain length beyond 10 was not beneficial to CR. Table S2 shows that C12-incorporated membrane has a lower CR than the C10-incorporated membrane. The solubility of C12 perfluoroalkyl phosphonic acid in both water and solvent is low, resulting in phase separation with Nafion™. This phase separation-related issue also appeared with FHPA (C12), which has a lower CR than PFOPA (C8). The phase segregation and solubility issues were further validated using phosphonated poly(styrene) (PWN), which has a CR of only 2.0% at FG/Ce=6. This result emphasizes the importance of insolubility in water and the compatibility of organic ligands with Nafion™ to obtain high CR. Polymeric phosphonic acids may be only effective when they are miscible with Nafion™. The results also highlight the importance of chain flexibility for high CR. PWN is a stiff polymer, and therefore phosphonic acid groups have limited ability to align around cerium ions. Flexibility could be another reason for the minimal CR of phosphonic acids below a certain length, although further investigation may need to be performed.

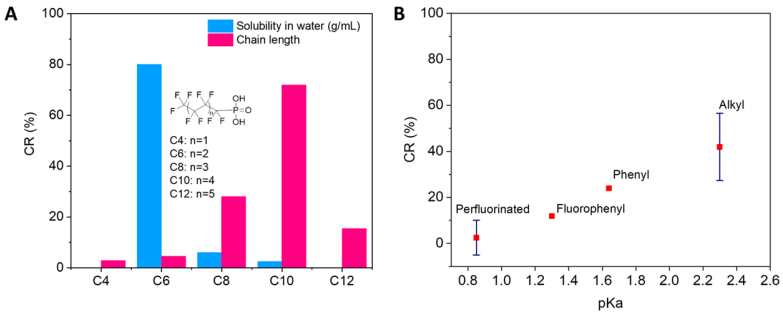

Figure 3. Substituent structural effects of phosphonic acid ligands

(A) Effect of chain length and ligand solubility on CR. (B) The effect of pK_a of phosphonic acids on CR. We used phosphonic acids with the number of carbon atoms between 4 and 8 per phosphonic acid and FG/Ce ratio of 4. Sample number is shown. All pK_a values except for 31 were calculated using the DFT approach in Supplementary Information.

Another notable structural effect of phosphonic acid ligands is pK_a. A phosphonic acid with lower pK_a dissociates protons more easily in water. In a mixture of acids, a proton from acid with a lower pK_a can transfer to the other acid with a higher pK_a.[34] Because Nafion™ is super acidic (pK_a = –6), the cerium cations that interact with the sulfate group in PFSA are easily dissociated in water. On the other hand, phosphonic acids, which are less acidic, form a more stable complex with cerium ions and thus, have a better ability to immobilize cerium ions. Because the CR takes place as an exchange process of a proton with a cerium cation, the equilibrium is likely controlled by the pK_a of the acids. To investigate the pK_a effect, we obtained the pK_a of several model phosphonic acids (pK_a = 0.8, 2.1-2.2[35]) and compared their CR with two prepared fluorophenyl phosphonic acids with different pK_a (1.20 and 1.64[36]) at FG/Ce=4 (Table S3, Figure 3B). The CR increased linearly with the pK_a of phosphonic acid in the experimental pK_a range. This is in alignment with the expectation that the stability of the complex should increase with the formation constant.[37] Namely, the expected order of cerium stability is: $R^fSO_3^-$ < $R^fP(O)(OM)(O)^-$ <$R^pP(O)(OM)(O)^-$ < $R^hP(O)(OM)(O)^-$ where R^f = perfluoroalkyl, R^p =phenyl, and R^h = alkyl. Relatively large variations in CR at a given pK_a were observed, suggesting that not only the basicity of the ligands but also the coordination stoichiometry and structural factors are crucial for the CR of cerium ions. The results also show that alkyl phosphonic acids are better ligands for higher CR than fluoro or phenyl phosphonic acids assuming compatibility with the polymer is acceptable. CR was found highest for Cyanex® 923, a mixture of phosphine oxides. The strong binding ability of phosphine oxides can be explained by the hard nature of ceric ions and O-donors, forming stable complexes.[37] The conjugate acids (R_3POH^+) are highly acidic and are likely in low concentration in this system where the acidity is largely leveled by the presence of water.[38]

To verify if the complex could indeed stabilize cerium against the potential conditions encountered during operation, a potential of 6 V was applied across the length of the membranes with alkyl phosphonic acids (PFOPA and FHPA) till the total charge transfer of 2C is achieved then the Ce concentration profile was evaluated. Figure 4 shows that the alkyl phosphonic acid incorporated membranes essentially eliminated the migration of cerium driven by potential gradients. In contrast, the baseline membrane exhibited cerium migrated to the cathodic potential. This result confirms the

ability of alkyl phosphonic acids as a stronger immobilizer for cerium under strongly acidic and potential gradient conditions.

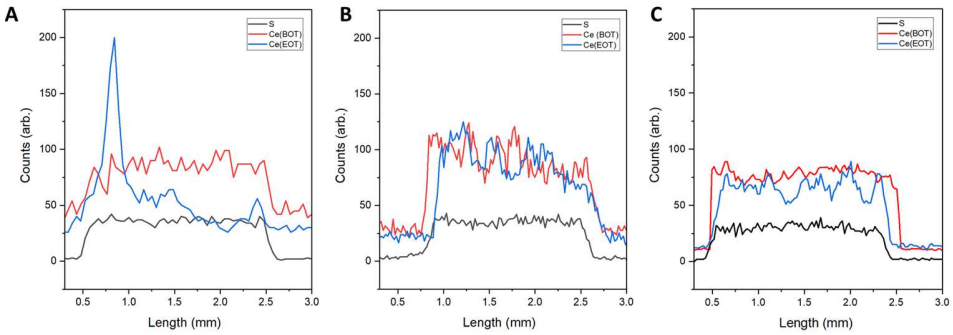

Figure 4. Cerium migration before and after potential test

The cerium profile across the (A) Ce-Nafion™ baseline membrane, (B) PFOPA-Ce-Nafion™ membrane, and (C) FHPA-Ce-Nafion™ membrane after applying potential of 6 V at 80 °C.

2.2 Effect of Ceric-ligand Complexes on Other Membrane Properties

2.2.1 Fluoride emission rate

An important question from the energetics study is whether the Ce-ligand complexation reduces the radical scavenging activity of cerium. To ensure this, we measured the fluoride emission rate (FER) of organic ligand-incorporated membranes under Fenton's test conditions (Figure 5a). The FER of the Nafion™ membrane without ceric ions was 0.85 $\mu g_F/g_{Nafion}$-hr. Incorporating ceric (1.8 wt%) into Nafion™ reduced FER to 0.39 $\mu g_F/g_{Nafion}$-hr. The FER for the 15C5 and A-15C5 incorporated Ce-Nafion™ membranes was 0.40 and 0.46 $\mu g_F/g_{Nafion}$-hr, respectively, comparable to the Ce-Nafion™ baseline membrane within the error limits. This suggests that the incorporation of the crown ether immobilizers does not inhibit the radical scavenging efficiency of cerium ions. Next, we evaluated the FER for phosphonic acid-incorporated membranes. Before assessing the FER of the phosphonic acid stabilized membranes, we tested the oxidative stability of phosphonic acids in Fenton's reagent to ensure no chemical structural changes of phosphonic acids under the testing conditions (Figure S1). The FER values for the PFOPA and C10 incorporated Ce-Nafion™ membranes were 0.24 and 0.37 $\mu g_F/g_{Nafion}$-hr, respectively, even lower than the Ce-Nafion™ baseline. This result suggests that phosphonic acids might have radical scavenging capability.[39] We further measured the FER of the PFOPA and C10 incorporated Ce-Nafion™ membranes as a function of the FG/Ce ratio (Figure 5b). The result shows that FER for the PFOPA-incorporated membrane gradually decreased as the phosphonic acid content increased. In contrast, the C10-incorporated membrane showed the opposite trend: the FER increases

with the higher content of C10 in the membrane. The different behavior could be due to the markedly different pK_a of the two ligands, which in turn, could be influencing the redox potential of cerium in ways that PFOPA is helping to scavenge radicals while C10 seems to be deterring it.[40] This result indicates that fluoroalkyl phosphonic acid (PFOPA) is a superior organic ligand to perfluoroalkyl phosphonic acid (C10) in terms of FER. We also evaluated the radical scavenging efficiency of the Cyanex® 923-incorporated membrane. To our surprise, the FER for the Cyanex® 923-immobilized membrane was much higher than for the unmodified Nafion™. The high FER generation rate is probably due to the generation of phosphorus-centered radicals in the presence of the Fenton's agent that could effectively disintegrate Nafion™.[41]

2.2.2 Proton conductivity

We further investigated the impact of organic ligands on the proton conductivity of the ligand-immobilized membranes (Figure 5c). The incorporation of organic ligands, except for C10 reduced the proton conductivity. The 15C5 showed slightly lower conductivity (19.5 S m^{-1}) than the baseline membrane (21.0 S m^{-1}). The A-15C5-immobilized membrane showed an additional 10% loss of conductivity (18.0 S m^{-1}) likely due to the interaction of amine groups with sulfonic acid side chains. The change in proton conductivity of the phosphonic acid-immobilized membranes depends on the pK_a and chemical structure. The proton conductivity of PFOPA and C10 incorporated membranes was 14.5 and 21.9 S m^{-1}, respectively. The conductivity of the Cyanex 923-immobilized membrane was significantly low (7.9 S m^{-1}) because of the tight complexation between the phosphine oxide and sulfonic acid group.[42]

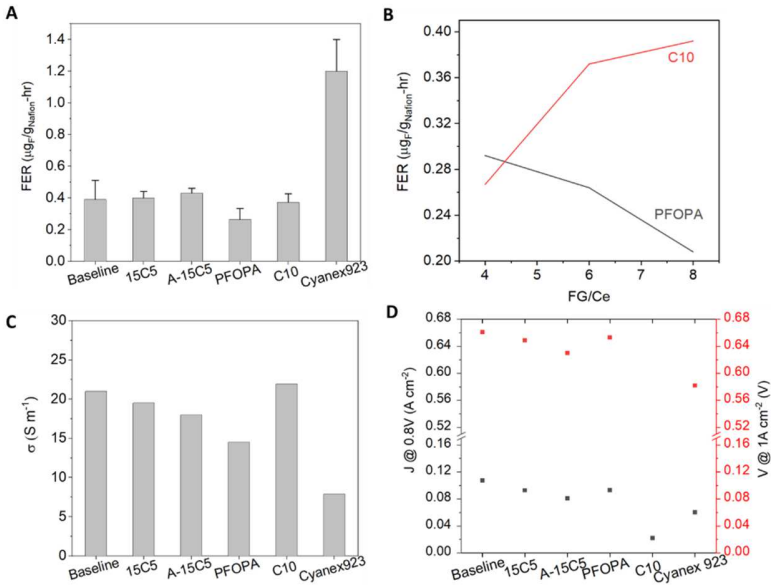

Figure 5. Impact of organic ligands on the properties of Ce-Nafion™ membranes

(A) FER of selected Ce-organic ligand complexes, (B) FER of PFOPA and C10 as a function of FG/Ce ratio, (C) Proton conductivity measured at 80 °C, in liquid water using the BekkTech cell. (D) Fuel cell performance measured at 0.8 V and 1 A cm^{-2}. The performance was measured at 80 °C under H_2/air conditions.

2.2.3 Membrane homogeneity

The homogeneity of the organic ligand-containing membranes was investigated with dispersion-cast membranes using scanning electron microscopy (Figure S2). The baseline membrane was transparent. The crown ether-incorporated membranes were clear despite the hydrocarbon nature of the ligand, likely due to the hydrophilicity induced by the cerium complex. Also, the small size and relatively low concentration of the crown ether contribute to good miscibility with Nafion™. The partially fluorinated phosphonic acid (PFOPA) incorporated membrane exhibited homogeneity, although the film was hazy, suggesting phase separation. Perfluorinated phosphonic acid (C10) immobilized membranes were clear and transparent. The alkyl di-phosphonic acid (PDPA) immobilized membrane showed white particles after casting, suggesting the phosphonic acid cerium complex could not be solubilized in Nafion. Cyanex® 923 caused gelation (Figure S3) due to the strong acid-base pair interaction of Nafion™ and phosphine oxide. During the evaporation process, notable amounts of phosphine oxides precipitated out, indicating the incompatibility between the long alkyl chains of the phosphine oxide and perfluorinated chains of Nafion™.

2.2.4 Catalyst poisoning

Another crucial requirement of organic ligands for fuel cell applications is the minimal poisoning of electrocatalysts. Although the organic cerium immobilizers are incorporated within the Nafion™ membrane, a small amount can migrate into the catalyst layers and reduce catalytic activity, i.e., catalyst poisoning. To evaluate the catalyst poisoning effect, we measured single-cell polarization curves using ligand-Ce-Nafion™ membranes (Figure S4). Figure 5d shows the current density of the MEAs at 0.8 V. The MEA using the baseline membrane showed a 6% current density loss compared to the MEA using unmodified Nafion™. The MEA using the 15C5 and A-15C5 incorporated membranes showed an additional 14% and 25% reduction in the current density, respectively. The A-15C5-incorporated MEA also had a higher loss in proton conductivity due to amine binding with the sulfonic acid sites. For all the phosphonic acid-incorporated membranes, a decrease in the current density at 0.8 V was observed likely due to phosphate adsorption on the Pt surface. The performance loss of the cell

using phosphonic acid ligands varies; the PFOPA-incorporated MEA showed relatively less current density reduction (13%) compared to the baseline cell, while the phosphonic acid with fluoroalkyl group (C10) exhibited considerable current density loss (80%). The current density reduction of the MEA with Cyanex® 923-incorporated membrane was notable (44%) likely due to the loss of sulfonic acid sites due to strong interactions. Catalyst poisoning by the organic ligands was also confirmed by the OCV losses measured during the testing (Figure S5). The MEA performance at the mass transport region measured at 1 A cm^{-2} exhibited a different behavior (Figure 5f). The performance loss of the MEAs using the 15C5 and PFOPA incorporated membranes was negligible, while notable performance loss for the MEAs using A-15C5, C10, and Cyanex® 923 incorporated membranes was observed. Considering that the electrochemical surface area loss of the C10 and Cyanex® 923 incorporated MEAs measured from the underpotentially-deposited hydrogen of the cyclic voltammograms was relatively small (Figure S6), the low mass transport performance of the MEAs using the C10 and Cyanex® 923 incorporated membranes is associated with the ligands that hinder reactant oxygen transport. The mass transport limit of the cell also affects its high-frequency resistance (Figure S7).

3. Conclusions

We investigated the use of organic immobilizers for mitigating cerium migration in PFSA-based PEMs. Although Cyanex® 923 composed of phosphine oxides was found to be the best immobilizing additive for cerium, degradation of PFSA accelerates in the presence of Cyanex® 923, making it unsuitable as a ceric immobilizer. Based on our investigation, phosphonic acids and crown ethers are two classes of ligands that show promise as viable solutions for cerium migration (Figure 6). The CR of phosphonic acids with a chain length of 8-10 is high. Particularly, alkyl phosphonic acids showed higher retention for ceric (45 times of baseline) than perfluorinated phosphonic acids with lower pK_a (36 times of baseline) due to the high pK_a of alkyl phosphonic acid. In addition, phosphonic acids themselves could aid the radical scavenging activity of ceric, further reducing fluoride emission by 38%. Therefore, alkyl phosphonic acids such as PFOPA and FHPA have a high potential to be the most effective immobilizer for ceric under acidic conditions. CR for crown ethers was found to be a strong function of the ring size. 15C5 was found to be the ideal size for cerium coordination. This size-driven immobilization does not show a strong negative influence on radical scavenging and performance while increasing membrane homogeneity for cerium incorporation. Although the crown ether showed lower CR than phosphonic acids, their benign and neutral nature makes crown ethers an interesting organic immobilizer for long-term fuel cell operation.

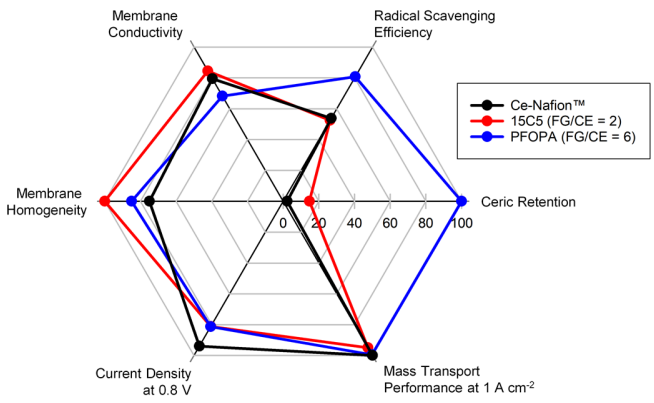

Figure 6. Comparison between 15C5 and PFOPA as a cerium immobilizer

The FG/Ce ratio for the 15C5 and PFOPA incorporated membranes are 2 and 6, respectively. The relative scale was made based on the highest value of each category from all tested membranes.

This study highlights the synchronous effect of phosphonic acid and crown ethers on their cerium radical scavenging potential by lowering fluoride emissions and preventing chemical degradation of membranes. We are looking into anchoring the screened ligands to PFSA to further enhance the stability of the complex and eliminate the potential migration of these small molecules during long-term fuel cell operation. Durability testing is currently ongoing to further confirm the cerium immobilization inducing enhanced durability of fuel cells.

4. Experimental procedures

4.1 Materials

Nafion™ D2020 was purchased from Ion Power, Inc. Diphenylphosphonic acid (DPA), (12-3,3,4,4,5,5,6,6,7,7,8,8,9,9,10,10,11,11,12,12,12-heneicosafluorododecyl) phosphonic acid (FHPA), octanediphosphonic acid (ODPA), 1H,1H,2H,2H-perfluorooctanephosphonic acid (PFOPA), fluorophenyl phosphonic acid (FPA), Rhodamine dye (RhB), ferrous sulfate, hydrogen peroxide 30 wt% solution, 12C4, 15C5, A-15C5, B-15C5, 18C6, melanin, melamine, tetraethyl ammonium hydroxide, tetramethyl ammonium hydroxide and dimethyl acetamide, perfluorohexyl iodide, perfluorooctyl iodide, perfluorodecyl iodide, isopropylmagnesium chloride (2.0 M in diethyl ether), diethyl chlorophosphate, and bromotrimethylsilane were purchased from Sigma Aldrich and used without further purification. Ceric sulfate tetrahydrate and 98% sulfuric acid were purchased from Fischer Scientific. Cyanex 923 was received from Solvay. Phosphonated poly(styrene) was supplied by Prof.

Vladimir Atanasov at the University of Stuttgart, Germany. (Octafluorobutyl)diphosphonic acid (C4DPA) was prepared according to a literature procedure.[43] Perfluoroalkyl phosphonic acids and BPA were synthesized in-house.

4.2 Material Synthesis

C4, C6, C8, C10, and C12 phosphonic acids were synthesized following a modified procedure reported in the literature.[44] The following is the procedure for the preparation of C8 perfluorophosphonic acid. To a 250-mL two-neck round bottom flask equipped with a magnetic stir bar were added perfluorooctyl iodide (5.0 g, 9.2 mmol) and anhydrous diethyl ether (46 mL) under an inert atmosphere at −45 °C. Isopropylmagnesium chloride solution (2.0 M in diethyl ether, 4.6 mL, 9.2 mmol, 1 eq.) was added to the mixture dropwise. After stirring at −45 °C for 1 h, diethyl chlorophosphate (1.6 g, 9.2 mmol, 1 eq.) was added, and the mixture was stirred at −45 °C for 1 h and at room temperature for 16 h. The reaction was quenched by adding 3.0 M HCl solution (4 mL, 12 mmol, 1.3 eq.) slowly. The organic layer was separated and dried over Na_2SO_4. After filtration and concentration, bromotrimethylsilane (2.9 g, 19 mmol, 2.1 eq.) was added slowly, and the mixture was stirred at room temperature for 12 h. After concentrating the reaction mixture using a rotary evaporator, water (10 mL) was added, and the mixture was stirred at room temperature for 12 h. The mixture was extracted with diethyl ether (3 × 40 mL), and the organic phase was collected and dried over Na_2SO_4. After filtration, diethyl ether was removed, and the crude product was obtained as a brown solid. The crude product (contains 30-50% unhydrolyzed phosphate ester) was further purified by treating with a large excess of concentrated HCl solution (100 mL, 36 wt%). The mixture was stirred under reflux for 24 hours. After cooling to room temperature, the mixture was diluted with distilled water (100 mL) and extracted by diethyl ether (3 × 100 mL). The ether phase was combined and dried over Na_2SO_4. After drying under reduced pressure at 60 ˚C overnight, the purified product was obtained as a brown solid (3.3 g, 73% yield). ^{1}H NMR (400 MHz, DMSO-d_6): δ (ppm) = 4.0 (m, 4H), 1.2 (m, 6H). ^{19}F NMR (376 MHz, DMSO-d_6): δ (ppm) = -80.4 (t, J = 9.6 Hz, 3F), -120.4 (m, 2F), -121.8 (m, 8F), -122.6 (m, 2F), -125.9 (m, 2F). ^{31}P NMR (162 MHz, DMSO-d_6): δ (ppm) -4.5 (t, J = 73.1 Hz) (Figure S8). C6, C10, and C12 perfluorophosphonic acids were prepared following the same procedures except using perfluorohexyl iodide, perfluorodecyl iodide, and perfluorododecyl iodide, respectively, as a reactant. The chemical structure of the C6, C8, and C10 were confirmed by ^{19}F-NMR and ^{31}P NMR (Figure S9). C8 before and after purification was characterized by ^{19}F NMR (Figure S10). The solubility of C6, C8, and C10 perfluorophosphonic acid in water was measured using the gravimetric method. The C12 perfluorophosphonic acid is insoluble in water and

only partially soluble in aprotic solvents, so we used the sample as synthesized without further characterization.

C6: 2.8 g, brown solid, 62% yield. ^{19}F NMR (376 MHz, DMSO-d_6): δ (ppm) = -80.4 (t, J = 9.7 Hz, 3F), -120.4 (m, 2F), -121.7 (m, 2F), -122.7 (m, 4F), -125.9 (m, 2F). ^{31}P NMR (162 MHz, DMSO-d_6): δ (ppm) -3.9 (t, J = 78.6 Hz).

C8: 3.3 g, brown solid, 73% yield. ^{19}F NMR (376 MHz, DMSO-d_6) δ (ppm) = -80.4 (t, J = 9.7 Hz, 3F), -120.4 (m, 2F), -121.5 (m, 2F), -121.9 (m, 4F), -122.6 (m, 2F), -122.9 (dt, J = 78.6, 13.6 Hz, 2F), -125.9 (m, 2F). ^{31}P NMR (162 MHz, DMSO-d_6): δ (ppm) -3.9 (t, J = 78.7 Hz).

C10: 3.5 g, brown solid, 76% yield. ^{19}F NMR (376 MHz, DMSO-d_6) δ (ppm) = -81.1 (m, 3F), -120.5 (m, 2F), -122.1 (m, 10F), -123.2 (m, 4F), -126.5 (m, 2F). ^{31}P NMR (162 MHz, DMSO-d_6): δ (ppm) -3.8 (t, J = 78.7 Hz).

Hexafluorobenzene (8.6 mmol) and anhydrous dimethylacetamide were added to a pressure vessel inside the glove box. Tris(trimethylsilyl) phosphite (17.2 mmol, 2 eq.) was added under N_2 atmosphere. The reaction mixture was heated to 165 °C for 4 h and then cooled to room temperature. The volatiles was removed under reduced pressure. The oil residue left in the bottom of the flask was poured into water. The mixture was boiled for 1 h under reflux, and the water was distilled to leave white crystals. The product (BPA) was dried under vacuum for 8 h. Yield 82%. No detectable peak was found in ^{1}H NMR. ^{19}F NMR (DMSO-d_6): -133.1 ppm (Figure S11).

4.3 Characterizations

4.3.1 Membrane casting

To 1 mL of 2-propanol/water solution, a calculated amount of ligand was added along with ceric sulfate tetrahydrate (0.22 mg), equivalent to 5 mole % of sulfonic acid groups of Nafion™. The mixture was stirred for 10 min. Then, Nafion™ dispersion D2020 (0.6g), was added to the mixture and the solution was diluted to 5 ml using 2-propanol/water mixture. The mixture was stirred at room temperature for 24 h. The membrane was cast in a casting tray at 80 °C overnight. The membranes were detached from the casting tray using hot water. The membrane thickness was ~50 µm.

4.3.2 Ceric retention accelerated stress test

To test ceric retention, the ceric content of the membrane at the beginning of the test was recorded using Thermo Scientific Quant'x EDXRF. The membranes were soaked in 0.5 M H_2SO_4 solution and then washed with water, gently dabbed using Kim wipes, and their ceric content was checked again after 24

h and 48 h of soaking.

4.3.3 Potential-driven ceric migration test

Membranes were cut into 1 cm × 3 cm pieces. The line scan of the membrane was recorded using EDAX ORBIS XRF at the beginning of the test. The membrane was then assembled into the BekkTech cell from Scribner and dipped in a beaker of water heated to 80 °C. 6 V of potential was then applied to the membrane. We do not control the time of the test but control the total charge transferred through all the membranes to be 2C. This ensures consistency across all the membranes. Depending on the conductivity of the membranes, the time varies and ranges from 45 minutes to 1 hour. After the test, the membrane was immediately taken out and dried using Kim wipes and the line scan was recorded to test the change in ceric distribution.

4.3.4 Proton conductivity

Proton conductivity was measured using BekkTech cell hardware. A 1 cm × 3 cm piece of the membrane was assembled into the BekkTech cell and dipped in a beaker of water at 80 °C. Linear sweep voltammetry was performed between 0.1 - 0.8V. The slope of the curve was recorded (in mA/V). Proton conductivity was then calculated using the formula,

$$\sigma\ (S/m) = 0.0425/(RWt)$$

where R is the resistance in Ω, W is the width in m, t is the thickness in m, and 0.0425 m is the distance between the working and the counter electrode.

4.3.5 FER measurement

FER is an ex-situ test wherein radicals are generated to attack the Nafion™ sites and thereby reduce the membrane weight over time. Fluoride anions emitted could be used as a measure of the degradation of Nafion™. Fenton solution contains 10 ppm Fe^{3+} ions along with 3 wt.% of H_2O_2 solution. The solution was changed every 24 h and replaced with a fresh solution. All the Fenton solution was collected to evaluate the fluoride concentration later using Thermo Scientific Dionex Ion Chromatography. The test was repeated with three different membranes and the average value was reported as the observed FER. Error bars show the maximum in the FER observed for each membrane.

4.3.6 Scanning electron microscopy

Images of the membrane surface were recorded by a high-resolution Quattro ESEM by Thermo Scientific at an accelerating voltage of 200 kV. The sample was cut into small pieces and attached to carbon paper during SEM imaging.

4.3.7 MEA fabrication and fuel cell testing

Nafion™ 212 was cut into small pieces and dissolved at 2.5 wt.% Nafion™ in dimethyl acetamide at 80 °C. A calculated amount of ligand was added to the Nafion™ solution along with 7.89 mg of ceric sulfate tetrahydrate. The solution was stirred for 24 h and then poured into a casting stay. The membrane was cast in a hot air oven at 80 °C for 6 h. It was then annealed in the hot air oven at 130 °C for 24 h. The membrane was then detached from the casting tray using hot water and used for testing without any further treatment.

As-synthesized catalysts were incorporated into the MEA by directly spraying a water/n-propanol-based ink onto a Nafion™ 211 membrane. The MEA with a geometric size of 5 cm^2 was prepared with a Pt loading of ~ 0.1 mg_{Pt} cm^2 on both the anode and cathode. We adopted a differential cell containing 14 parallel flow channels in our testing. The MEA was sandwiched between two graphite plates with straight parallel flow channels machined in them. The cell was operated at 80 °C, with 150 kPa_{abs} H_2/air and a gas flow rate of 500/1000 sccm for anode/cathode, respectively. Seven break-in cycles were run before recording the performance and the CV for the various membranes. The electrochemical active surface area (ECSA) was obtained by calculating H_{UPD} charge in CV curves between 0.1 - 0.4 V (0.4 - 0.45 V background subtracted); assuming a value of 210 μC cm^{-2} for the adsorption of a hydrogen monolayer on Pt (CV curves were obtained under 150 kPa_{abs} H_2/N_2, 30 °C, > 100 % RH, 500/1000 sccm).

4.3.8 DFT calculations

All DFT calculations were performed using the Gaussian16 quantum chemistry package. For the calculation of interaction energies, the B3LYP/6-31G(d) level of theory was used for C, H, P, O, and F atoms.[45] For the description of Ce^{4+} we used Stuttgart-Dresden relativistic effective core potential MWB 28 together with the corresponding optimized valence basis set.[46-48] The structures of the ligands were first optimized and the optimized geometries were used for predicting the complex structure of the ligands coordinated to ceric ion. The interaction energies were calculated using optimized structures of Ce^{4+}-ligand complexes using the formulae:

$$E_{int} = E(Ce^{4+}\text{-crown}) - [E(Ce^{4+}) + E(\text{crown})]$$

$$E_{int} = E(Ce^{4+}\text{-}\ n\ \text{PA}) - [E(Ce^{4+}) + E(n\ \text{PA})$$

When water molecules were coordinated to Ce^{4+} at the same time as the functional phosphoric acids, the interaction energy was defined as

$$E_{int} = E(Ce^{4+}\text{-}\ n\ \text{PA-water}) - [E(Ce^{4+}) + E(n\ \text{PA-water})$$

All values were corrected for basis set superposition errors using the counterpoise method.[49, 50] [50]

The pK_a values of (fluoro-)phosphonic acids were obtained using the previously established procedure that relies on the linear regression fit of the experimentally known pK values to the DFT calculated deprotonation energies. The details of the procedure are given in Ref.[34]. Deprotonation energies ($E_{A^-} - E_{HA}$), calculated using SMD model[51] at the M06L/6-311++G(d,p) level of theory[52], are 280.17 (PFOPA), 281.04 (ODPA), 281.07 (PDPA), 268.57 (C4), 268.31 (C6), 268.46 (C8), and 272.48 (BPA) kcal mol^{-1} resulting in pK_a of 2.1 (PFOPA), 2.2 (ODPA), 2.2 (PDPA), 0.8 (C4), 0.8 (C6), 0.8 (C8) and 1.2 (BPA).

Acknowledgment

We thank Prof. Vladimir Atanasov for providing the PWN ionomer. The US Department of Energy (US DOE), Office of Energy Efficiency and Renewable Energy (EERE), and Hydrogen and Fuel Cell Technologies Office (HFTO) supported this research through the M2FCT (Million Mile Fuel Cell Truck) Consortium. Material synthesis efforts were supported by US DOE Advanced Research Projects Agency-Energy (Award number: DE-AR0001003). I. M. acknowledges access to the computational resources of LANL Institutional Computing Program, which is supported by the US Department of Energy National Nuclear Security Administration under contract 89233218CNA000001, NERSC, a DOE Office of Science User Facility supported by the Office of Science of the US Department of Energy under contract DE-AC02-05CH11231, and CARC, UNM Center for Advanced Research Computing.

References

[1] C.S. Gittleman, H.F. Jia, E.S. De Castro, C.R.I. Chisholm, Y.S. Kim, Joule, 5 (2021) 1660-1677.

[2] D.A. Cullen, K.C. Neyerlin, R.K. Ahluwalia, R. Mukundan, K.L. More, R.L. Borup, A.Z. Weber, D.J. Myers, A. Kusoglu, Nature Energy, 6 (2021) 462-474.

[3] M. Zaton, J. Roziere, D.J. Jones, Sustain Energ Fuels, 1 (2017) 409-438.

[4] R. Borup, J. Meyers, B.S. Pivovar, Y.S. Kim, R. Mukundan, N. Garland, D. Myers, M. Wilson, F. Garzon, D. Wood, P. Zelenay, K.L. More, K. Stroh, T.A. Zawodzinski, J. Boncella, J.E. McGrath, M. Inaba, K. Miyatake, M. Hori, K. Ota, Z. Ogumi, S. Miyata, A. Nishikata, Z. Siroma, Y. Uchimoto, K. Yasuda, K.I. Kimijima, N. Iwashita, Chem Rev, 107 (2007) 3904-3951.

[5] E. Endo, J. Mukoyama, JP2006260811A, 2005.

[6] T. Tanuma, T. Itoh, Journal of Power Sources, 305 (2016) 17-21.

[7] F.D. Coms, H. Liu, J.E. Owejan, ECS Transactions, 16 (2008) 1735-1747.

[8] A.M. Baker, R. Mukundan, D. Spernjak, S.G. Advani, A.K. Prasad, R.L. Borup, Polymer Electrolyte Fuel Cells 16 (Pefc 16), 75 (2016) 707-714.

[9] M. Zaton, B. Prelot, N. Donzel, J. Roziere, D.J. Jones, J Electrochem Soc, 165 (2018) F3281-F3289.

[10] S.M. Stewart, D. Spernjak, R. Borup, A. Datye, F. Garzon, Ecs Electrochem Lett, 3 (2014) F19-F22.

[11] A.M. Baker, S.K. Babu, R. Mukundan, S.G. Advani, A.K. Prasad, D. Spernjak, R.L. Borup, J Electrochem Soc, 164 (2017) F1272-F1278.

[12] Y.H. Lai, K.M. Rahmoeller, J.H. Hurst, R.S. Kukreja, M. Atwan, A.J. Maslyn, C.S. Gittleman, J Electrochem Soc, 165 (2018) F3217-F3229.

[13] D. Banham, S.Y. Ye, T. Cheng, S. Knights, S.M. Stewart, M. Wilson, F. Garzon, J Electrochem Soc, 161 (2014) F1075-F1080.

[14] A.M. Baker, S.T.D. Williams, R. Mukundan, D. Spernjak, S.G. Advani, A.K. Prasad, R.L. Borup, J Mater Chem A, 5 (2017) 15073-15079.

[15] N. Ramaswamy, in: US DOE Hydrogen and Fuel Cells Program: 2020 Annual Merit Review and Peer Evaluation Report, 2020, https://www.hydrogen.energy.gov/pdfs/review20/fc323_ramaswamy_2020_p.pdf.

[16] A.M. Baker, S.M. Stewart, K.P. Ramaiyan, D. Banham, S.Y. Ye, F. Garzon, R. Mukundan, R.L. Borup, J Electrochem Soc, 168 (2021) 024507.

[17] D.C. Seo, I. Jeon, E.S. Jeong, J.Y. Jho, Polymers-Basel, 12 (2020) 1375.

[18] M. Vinothkannan, S. Ramakrishnan, A.R. Kim, H.K. Lee, D.J. Yoo, Acs Appl Mater Inter, 12 (2020) 5704-5716.

[19] A. Akrout, A. Delrue, M. Zaton, F. Duquet, F. Spanu, M. Taillades-Jacquin, S. Cavaliere, D. Jones, J. Roziere, Membranes-Basel, 10 (2020).

[20] V.D.C. Tinh, D. Kim, J Membrane Sci, 613 (2020) 118517.

[21] A. Kodir, S.H. Shin, S. Park, M.R. Arbi, T.H. Yang, H. Lee, D. Shin, B. Bae, Int J Energ Res, 46 (2021) 7186-7200.

[22] A. Kodir, S.H. Shin, S. Park, M.R. Arbi, T.H. Yang, H. Lee, D. Shin, B. Bae, Int J Energ Res, 46 (2022) 7186-7200.

[23] T. Agarwal, Allen Sievert, Siddharth Komini Babu, Santosh Adhikari, Ajay K. Prasad, Suresh G. Advani, Timothy Hopkins, Andrew Park, Yu Seung Kim, and Rod Borup., Available at SSRN 4172909., (2022).

[24] H.F. Aly, S.M. Khalifa, J.D. Navratil, M.T. Saba, Solvent Extr Ion Exc, 3 (1985) 623-636.

[25] C.M. Choi, J. Heo, N.J. Kim, Chem Cent J, 6 (2012) 84.

[26] R.X. Mu, J. Chen, D. Zou, K. Li, D.Q. Li, Sep Purif Technol, 209 (2019) 351-358.

[27] Y. Liu, B.H. Han, Y.T. Chen, Coordin Chem Rev, 200 (2000) 53-73.

[28] A.M. Wilson, P.J. Bailey, P.A. Tasker, J.R. Turkington, R.A. Grant, J.B. Love, Chem Soc Rev, 43 (2014) 123-134.

[29] Z. Li, B. Dewulf, K. Binnemans, Ind Eng Chem Res, 60 (2021) 17285-17302.

[30] M.R. Awual, T. Yaita, H. Shiwaku, Chem Eng J, 228 (2013) 327-335.

[31] A.S. Lee, Y.K. Choe, I. Matanovic, Y.S. Kim, J Mater Chem A, 7 (2019) 9867-9876.

[32] I. Matanovic, A.S. Lee, Y.S. Kim, J Phys Chem B, 124 (2020) 7725-7734.

[33] I. Matanovic, A.S. Lee, Y.S. Kim, J Phys Chem B, 124 (2020) 7725-7734.

[34] K.H. Lim, A.S. Lee, V. Atanasov, J. Kerres, S. Adhikari, S. Maurya, E.J. Park, L.D. Manriquez, J. Jung, C. Fujimoto, I. Matanovic, J. Jankovic, Z. Hu, H. Jia, Y.S. Kim, Nature Energy, 7 (2022) 248-259.

[35] S.M. Zhang, J Comput Chem, 33 (2012) 2469-2482.

[36] S.M. Zhang, J. Baker, P. Pulay, Journal of Physical Chemistry A, 114 (2010) 425-431.

[37] V.V. Grushin, Chem Rev, 104 (2004) 1629-1662.

[38] C.H. Wang, A. Robertson, R.G. Weiss, Langmuir, 19 (2003) 1036-1046.

[39] H.Y. Chen, Acs Omega, 4 (2019) 14105-14113.

[40] T. Kwon, S.H. Park, B.J. Min, S. Park, S. Ramadhani, Y. Lim, S.S. Jang, H. Jeong, H.J. Son, J.Y. Kim, Adv Energy Sustainability, (2022) 2200011.

[41] C. Bellanger, S. Chelli, S. Lakhdar, Phosphorus-Centered Radicals, in: C. Ollivier, L. Fensterbank (Eds.) Free Radicals: Fundamentals and Applications in Organic Synthesis 1, 2021, pp. 227-272.

[42] Y.S. Kim, B.R. Einsla, M. Sankir, W. Harrison, B.S. Pivovar, Polymer, 47 (2006) 4026-4035.

[43] H.K. Nair, D.J. Burton, Tetrahedron Lett, 36 (1995) 347-350.

[44] M.B. Herath, S.E. Creager, A. Kitaygorodskiy, D.D. DesMarteau, J Phys Chem B, 114 (2010) 14972-14976.

[45] M.J. Frisch, G.W. Trucks, H.B. Schlegel, G.E. Scuseria, M.A. Robb, J.R. Cheeseman, G. Scalmani, V. Barone, B. Mennucci, G.A. Petersson, M. Nakatsuji, X. Caricato, H.P. Li, A.F. Hratchian, J. Izmaylov, G. Bloino, J.L. Zheng, M. Sonnenberg, M. Hada, K. Ehara, R. Toyota, J. Fukuda, M. Hasegawa, T. Ishida, Y. Nakajima, O. Honda, H. Kitao, T. Nakai, J.A. Vreven, J. Montgomery, J. E. , F. Peralta, M. Ogliaro, J.J. Bearpark, E. Heyd, K.N. Brothers, V.N. Kudin, R. Staroverov, J. Kobayashi, K. Normand, A. Raghavachari, J.C. Rendell, S.S. Burant, J. Iyengar, M. Tomasi, N. Cossi, J.M. Rega, M. Millam, J.E. Klene, J.B. Knox, V. Cross, C. Bakken, J. Adamo, R. Jaramillo, R.E. Gomperts, O. Stratmann, A.J. Yazyev, R. Austin, C. Cammi, J.W. Pomelli, R.L. Ochterski, K. Martin, V.G. Morokuma, G.A. Zakrzewski, P. Voth, J.J. Salvador, S. Dannenberg, A.D. Dapprich, Ö. Daniels, J.B. Farkas, J.V. Foresman, J. Ortiz, J. Cioslowski, D.J. Fox, Gaussian 09, Revision B.01; Gaussian, Inc.: Wallingford, CT, (2009).

[46] M. Dolg, P. Fulde, W. Kuchle, C.S. Neumann, H. Stoll, J Chem Phys, 94 (1991) 3011-3017.

[47] M. Dolg, H. Stoll, H. Preuss, J Chem Phys, 90 (1989) 1730-1734.

[48] X.Y. Cao, M. Dolg, J Chem Phys, 115 (2001) 7348-7355.

[49] S.F. Boys, F. Bernardi, Mol Phys, 19 (1970) 553-566.

[50] S. Simon, M. Duran, J.J. Dannenberg, J Chem Phys, 105 (1996) 11024-11031.

[51] A.V. Marenich, C.J. Cramer, D.G. Truhlar, J Phys Chem B, 113 (2009) 6378-6396.

[52] Y. Zhao, D.G. Truhlar, Theor Chem Acc, 120 (2008) 215-241.

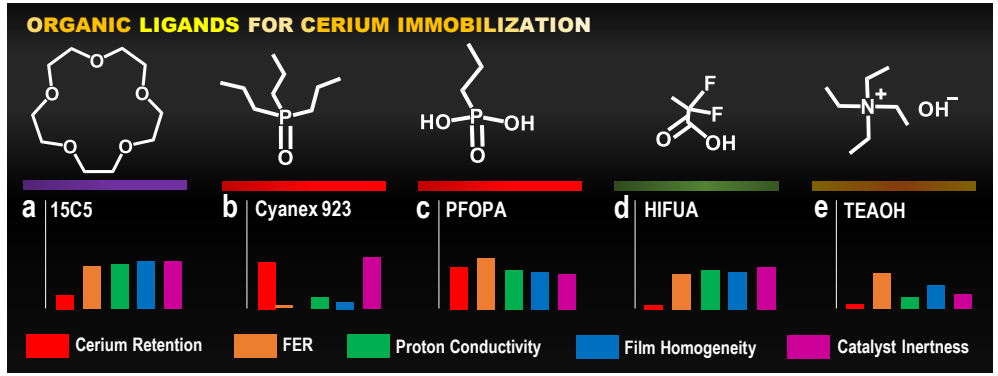
ORGANIC LIGANDS FOR CERIUM IMMOBILIZATION
a 15C5
b Cyanex 923
c PFOPA
d HIFUA
e TEAOH
Cerium Retention
FER
Proton Conductivity
Film Homogeneity
Catalyst Inertness